Test of a Planetary Boundary-Layer Parameterization Based on a Generalized Similarity Theory in Tropical Cyclone Models

SIMON WEI-JEN CHANG[1]

JAYCOR, Alexandria, VA 22304

(Manuscript received 8 April 1980, in final form 18 October 1980)

ABSTRACT

A planetary boundary-layer (PBL) parameterization based on the generalized similarity theory (GST) was tested in tropical cyclone models. This parameterization, with only one layer, is desired in modeling tropical cyclones for computational speed. The momentum, sensible heat and moisture fluxes are mutually dependent in this parameterization through nondimensional gradient equations. The internal structure of the PBL is determined implicitly through universal functions.

In comparison with a complex, one-dimensional, multilayer PBL model, the GST parameterization yields accurate moisture fluxes, but slightly overestimates the momentum flux and underestimates the sensible heat flux. The GST parameterization produces very realistic dynamics, energetics and thermal structure in an axisymmetric tropical cyclone model. This GST parameterization, although unable to treat the diffusion across the PBL inversion, is judged superior to drag coefficient parameterization and is a good alternative to the more expensive, multilayer parameterization.

1. Introduction

The planetary boundary layer (PBL) plays a critical role in the evolution of tropical cyclones because the air-sea energy and momentum exchanges occur through the PBL. Parameterization of the PBL is thus a very important aspect of tropical cyclone modeling. Complex parameterization is not always computationally feasible for three-dimensional or operational models. Computationally efficient yet accurate PBL parameterization is imperative for these models. The purpose of this paper is to test such a parameterization based on the generalized similarity theory (GST) in the parameterization of the PBL in tropical cyclone models.

The most widely used PBL model is the single-layer parameterization where the PBL is represented by one model layer and the surface fluxes are calculated using bulk aerodynamic formulas. This method is simple and computationally economical but has a major drawback in that the internal structure of the PBL cannot be resolved. As a consequence, the single-layer PBL model using bulk aerodynamic formulas can only crudely estimate various surface fluxes.

An alternative approach where the PBL is modeled by several layers has been adopted in recent years by Pielke (1974), Kurihara and Tuleya (1974), Anthes and Chang (1978) and Anthes and Warner (1978). By explicitly resolving the PBL structure, these models often yield more realistic estimates of the various fluxes, but the computational cost is high.

Recent observational studies have facilitated the testing of various PBL similarity theories. The rather idealized assumptions characteristic of early theories have been relaxed and improved, and more realistic and general theories have been derived (Arya, 1977; Yamada, 1976). These developments have led to a PBL formulation that appears suitable to model various PBL conditions. The purpose of this study is to examine the viability of such formulation in tropical cyclone models.

In the next section, a brief review of the generalized similarity theory will be given. In Section 3, various surface fluxes in typical tropical cyclone conditions obtained from the GST will be compared with those computed by a time dependent one-dimensional PBL model (Busch, *et al.*, 1976; hereafter referred as BCA). The generalized similarity theory is then applied to an axisymmetric tropical cyclone model. The results will be compared in Section 4 with those obtained using constant drag coefficients.

2. Generalized similarity theory

Similarity theory states that the profile of any properly scaled variable in the PBL such as wind, temperature or water vapor can be described by a universal function. Although there has been much debate concerning the proper scales for the various

[1] Current affiliation: Science Applications, Inc., McLean, VA 22102.

0027-0644/81/040843-11$06.75

TABLE 1. Model used for comparison.

Models	Type	Dimensions	PBL parameterization
GST	PBL	1	Single-layer generalized similarity theory
BCA	PBL	1	Multilayer (Busch *et al.*, 1976)
S	Tropical cyclone	2	Single-layer, generalized similarity
D1	Tropical cyclone	2	Single-layer, $C_D = 0.0015$, $C_E = C_H = 0.003$
D2	Tropical cyclone	2	Single-layer, $C_D = 0.003$, $C_E = C_H = 0.003$
M	Tropical cyclone	2	Multilayer (Busch *et al.*, 1976)

types of PBL's (Arya, 1977) we will use a similarity theory that appears most applicable and general for tropical cyclones (Yamada, 1976).

The mathematical representation of the PBL flow can be obtained by assuming that there exists a layer where both the equations describing the surface layer and the equations describing the interior flow in the mixed layer are both valid. In the surface layer, the PBL variables are assumed to follow a logarithmic-linear relationship with height:

$$\mathbf{t}\frac{|\mathbf{v}|}{u_*} = \frac{\mathbf{t}}{k}\left[\ln\left(\frac{z}{z_0}\right) - \Psi_m\left(\frac{z}{Z}\right)\right], \tag{1a}$$

$$\frac{\theta - \theta_0}{\theta_*} = \frac{\mathrm{Pr}}{k}\left[\ln\left(\frac{z}{z_0}\right) - \Psi_h\left(\frac{z}{L}\right)\right], \tag{1b}$$

$$\frac{q - q_0}{q_*} = \frac{\mathrm{Pr}}{k}\left[\ln\left(\frac{z}{z_0}\right) - \Psi_q\left(\frac{z}{L}\right)\right], \tag{1c}$$

where $\mathbf{t}$ is the unit vector parallel to the surface wind, Pr is the turbulent Prandtl number, Ψ_m, Ψ_h and Ψ_q are stability functions, z_0 is the roughness length, and θ_0 and q_0 are potential temperature and specific humidity at z_0.

For the interior flow in the mixed layer we can write the equations in the form of the resistance law:

$$\frac{\mathbf{V} - \mathbf{V}_m}{u_*} = \mathbf{t}F_u\left(\frac{z}{h}, \frac{h}{L}\right) + \mathbf{n}F_v\left(\frac{z}{h}, \frac{h}{L}\right)\mathrm{sign}\, f, \tag{2a}$$

$$\frac{\theta - \theta_m}{\theta_*} = F_\theta\left(\frac{z}{h}, \frac{h}{L}\right), \tag{2b}$$

$$\frac{q - q_m}{q_*} = F_q\left(\frac{z}{h}, \frac{h}{L}\right), \tag{2c}$$

where $\mathbf{V}_m$, θ_m and q_m are the mean velocity, potential temperatures and water vapor content in the PBL, $\mathbf{n}$ is a unit vector normal to $\mathbf{t}$, h is the height of the PBL, and F_u, F_v, F_θ and F_q are functions to be determined.

Assuming a matching layer where (1) and (2) are simultaneously valid, one can obtain a relation between the surface fluxes and the average PBL parameters:

$$\frac{ku_m}{u_*} = \ln\left(\frac{h}{z_0}\right) - A\left(\frac{h}{L}\right), \tag{3a}$$

$$\frac{kv_m}{u_*} = -B\left(\frac{h}{L}\right)\mathrm{sign}\, f, \tag{3b}$$

$$\frac{k(\theta_0 - \theta_m)}{\mathrm{Pr}\theta_*} = \ln\left(\frac{h}{z_0}\right) - C\left(\frac{h}{L}\right), \tag{3c}$$

$$\frac{k(q_0 - q_m)}{\mathrm{Pr}q_*} = \ln\left(\frac{h}{z_0}\right) - D\left(\frac{h}{L}\right), \tag{3d}$$

where u_m and v_m are the components of the mean velocity in the PBL in the $\mathbf{t}$ and $\mathbf{n}$ directions, respectively. Universal functions A, B, C and D are determined empirically. It is generally assumed that $D \approx C$ (see Arya, 1977).

Using equation set (3), and the Wagara observational data, Yamada (1976) obtained functions A, B and C [Eqs. (13)–(18) in his paper] which are adopted here because of the simple functional form and accuracy.

It should be noted that $\mathbf{V}_m$ in Yamada's analysis is the vertically averaged geostrophic wind in the PBL. Here $\mathbf{V}_m$ is the vertically averaged mean wind. Thus the baroclinic effects are minimized (Arya, 1978). In addition, when actually applying Eq. (3) in a dynamic model, the sum of the squares and the quotients of Eqs. (3a) and (3b) are used to evaluate the magnitude and direction of the surface wind stress.

3. Generalized similarity theory and multilayer approaches in a one-dimensional tropical cyclone model

As stated in the Introduction, the parameterization of the PBL based on the GST for a tropical cyclone model is very appealing because it requires only one layer to represent the PBL. Thus, it is important to test the universal functions described by Eq. (3) with the observations of tropical cyclones. Unfortunately, detailed observations of tropical cyclone PBL's are not yet available, so we resort to use a one-dimensional, multilayer PBL model for comparison. Table 1 lists various models used in this study.

The BCA one-dimensional PBL model can reproduce observations accurately and it has been used successfully in parameterizing the PBL in numerical models (Anthes and Chang, 1978; Anthes *et al.*, 1978). The model has a surface layer in which the logarithmic-linear relationships for wind and temperature (Businger *et al.*, 1971) are adopted. It should be noted that the same logarithmic-linear relation-

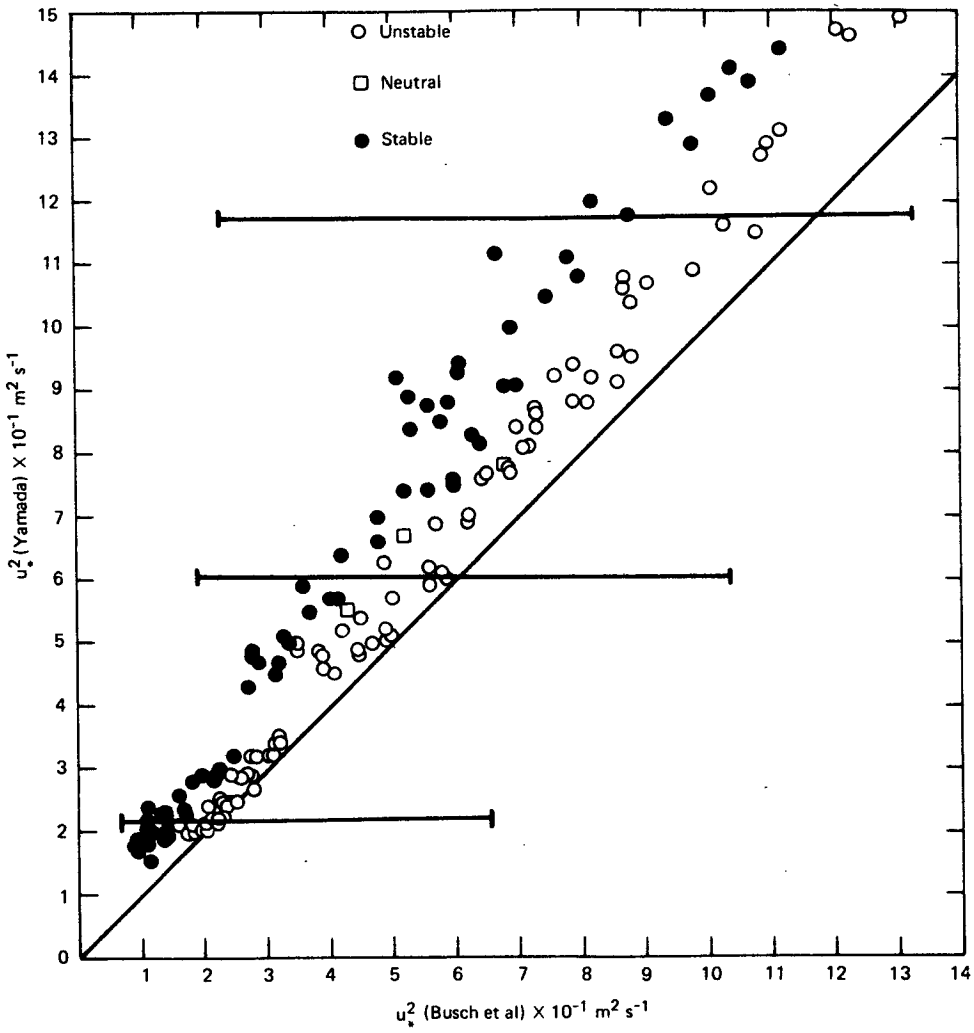

FIG. 1. Surface stresses (m^2 s^{-1}) computed by generalized similarity theory versus those computed by the one-dimensional PBL model for stable (●), unstable (○), and neutral (□) conditions. Points should fall on the diagonal line if two models agree.

ship is used by Yamada (1976) to generate the universal functions. Above the surface layer, a time-dependent mixing length is used. The mixing length is assumed to continuously approach its asymptotic value, which depends on the depth and stability of the PBL. The *e*-folding time of the mixing length is proportional to the size of the energy-containing eddies in the PBL and inversely proportional to the turbulent kinetic energy.

The one-dimensional version of the BCA model used in this study has 20 layers using a stretched grid from the surface to 3 km. The lowest layer defined as the surface layer, has a thickness of 25 m. To properly simulate tropical cyclone condition, a rather strong pressure gradient force is specified so that the geostrophic wind speed is strongest at the surface and decreases with height to 90% of its surface strength at 3 km. The initial thermal state which has been taken from the model hurricane of Anthes and Chang (1978) shows a well-mixed PBL below a capping inversion at 600 m with a sharp increase of potential temperature and decrease of specific humidity above the inversion. The initial wind is equal to the geostrophic wind prescribed for each run.

The BCA model was integrated 12 h for 24 cases with the values of the geostrophic wind set at 15, 25 and 35 m s^{-1} and the sea-surface temperature (SST) varying from 24.4 to 29.4°C. These variations produce different stability conditions and large rates of change in the initial hours. Diagnoses using Eq. (3) (or the GSA model) were given at model times of 1, 2, 3, 4, 6, 8 10 and 12 h. The vertically integrated u, v, θ and q in the BCA model are the mean PBL properties needed for the diagnoses. Fig. 1 shows the comparison of the surface wind stresses between the diagnoses from GST model and the computation of BCA model. The GST model produced nearly the same results (points on the diagonal line in Fig. 1)

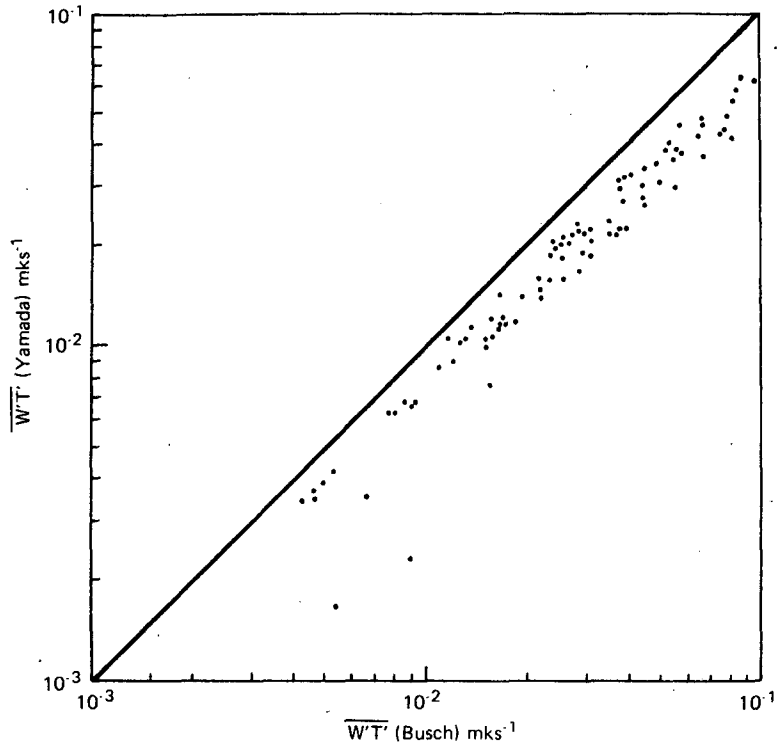

FIG. 2. As in Fig. 1 except for upward surface heat flux in unstable condition (°C m s^{-1}).

as the BCA model for small u_*^2 value and for the unstable conditions. The stress diagnosed by the GST are higher than the BCA model under stable conditions. The overestimate by the GST model lessens as instability increases.

The larger estimation of the surface stresses for stable conditions of the GST model is due to the greater wind shear in the lower PBL which is resolvable in the BCA model. This strong wind shear is not properly represented by the universal functions in the single-layer approach. When such a strongly sheared layer, which usually accompanies a low-level inversion, is present, the PBL mean wind may not be a proper velocity scale for the PBL. Fortunately, the formation of such a low-level inversion is not likely in tropical cyclones, the GST model therefore seems to estimate the momentum fluxes in typical tropical cyclones quite well.

We also used a constant aerodynamic drag coefficient of 1.5×10^{-3} to estimate the stresses due to surface winds from the BCA model. Because the drag coefficient is independent of stability, the value of the stresses depends strongly on the wind speed. A comparison with BCA model shows that most of the values cluster along the three horizontal lines and scatter within the vertical bars on two ends of each line in Fig. 1. These scattering and clustering points are also typical for the drag coefficient model in heat flux and moisture flux. It is apparent that the stresses of the GSA model have more correlation and less scattering to those of the more sophisticated BCA model as compared to the aerodynamic drag coefficient model.

Figs. 2 and 3 show the comparisons of the upward and downward sensible heat fluxes, respectively. For unstable conditions, the GST model underestimates the upward heat flux because of the formation of a strong superadiabatic lapse rate region near the surface in the BCA model. For stable conditions the GST model overestimates the downward heat flux. This is related to the formation of low-level inversion in the BCA model which effectively cuts off the downward transport of heat. These characteristics of the GST model are found in almost all single-layer parameterizations because the strong gradient in lower PBL cannot be resolved. This difficulty cannot be easily overcome when a single-layer PBL has to be employed in a numerical model for economic reasons.

Fig. 4 shows the comparison of the moisture flux $\overline{w'q'}$. The GST model gives a higher $\overline{w'q'}$ for the unstable condition, and a very similar $\overline{w'q'}$ for near neutral conditions, and scattering in Fig. 4 is similar to that in Fig. 1, the more symmetric distribution

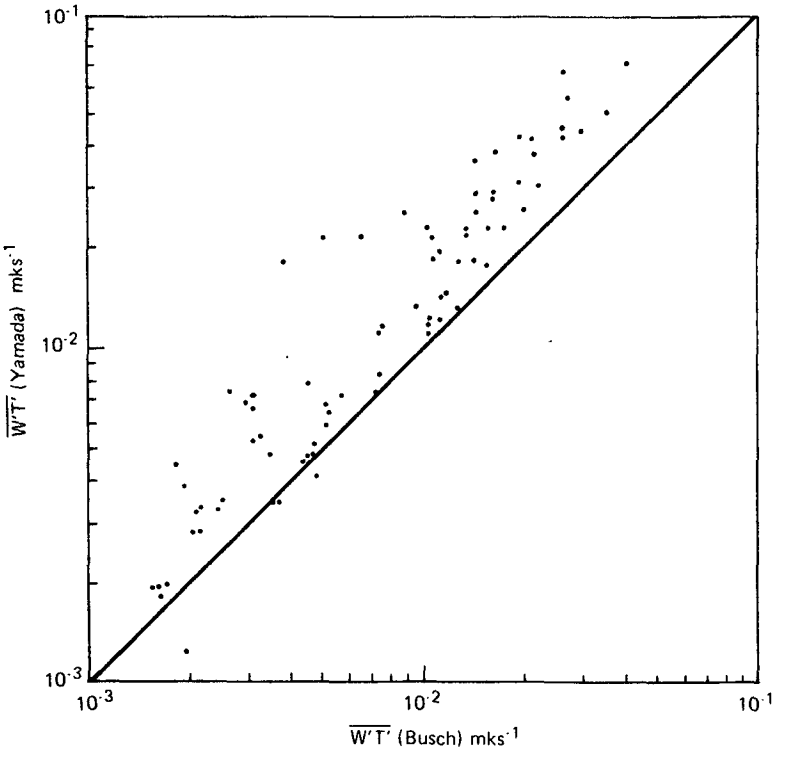

FIG. 3. As in Fig. 1 except for downward surface heat flux in stable conditions (°C m s^{-1}).

about the diagonal in Fig. 4 is presumably related to the larger value of $\partial q/\partial z$ in the lower part of the BCA model.

These deviations of the GST model from the BCA model are much less than the model using aerodynamic drag coefficients. Using a constant drag coefficient, various fluxes depend almost solely on the wind speed. The deviations of the GST model from the BCA model is partially inherited from the scattering of the original observation data from which the universal functions are deduced (Yamada, 1976). The comparison, however, does indicate a distinct behavior of the GST model for different stability. It should be pointed out that the GST has been applied to highly nonstationary conditions in this analysis. We note that as the PBL approaches a quasi-steady state, the GST model diagnoses becomes comparable to the BCA model results.

The experiments with the one-dimensional model indicates that the GST model agrees very well with the Busch model in momentum and moisture flux predictions. The GST model does not predict accurate fluxes when there are strong low-level gradients of potential temperature. The surface heat flux, however, is fortuitously not critically important in the development and maintenance of tropical cyclones as pointed out by Rosenthal (1971) and Anthes and Chang (1978). The single-layer approach with GST model in parameterizing the PBL in a tropical cyclone is thus adequate.

4. Incorporation with an axisymmetric tropical cyclone model

a. Model review

The axisymmetric tropical cyclone model used for our investigation is similar to the one described in Anthes and Chang (1978) except that (1) the finest resolution at small radii is 30 km, and (2) there are six vertical layers. The vertical σ layers are bounded at levels σ = 0.0, 0.2, 0.3, 0.6, 0.8, 0.93 and 1.

Included in one earlier version of the model was a time dependent equation for the PBL height similar to that in Deardorff (1972). Supplementary experiments showed that the equation predicts infinite growth of PBL near the center of the cyclone unless large horizontal diffusion is applied. We, therefore, hold the height of PBL constant between σ = 0.93 and 1. The PBL has a depth of 650 = 700 m, a typical observed PBL depth near tropical disturbances (Moss and Merceret, 1976). Charnock's equation (Delsol *et al.*, 1970) is used to compute the roughness length. The initial conditions consist of a

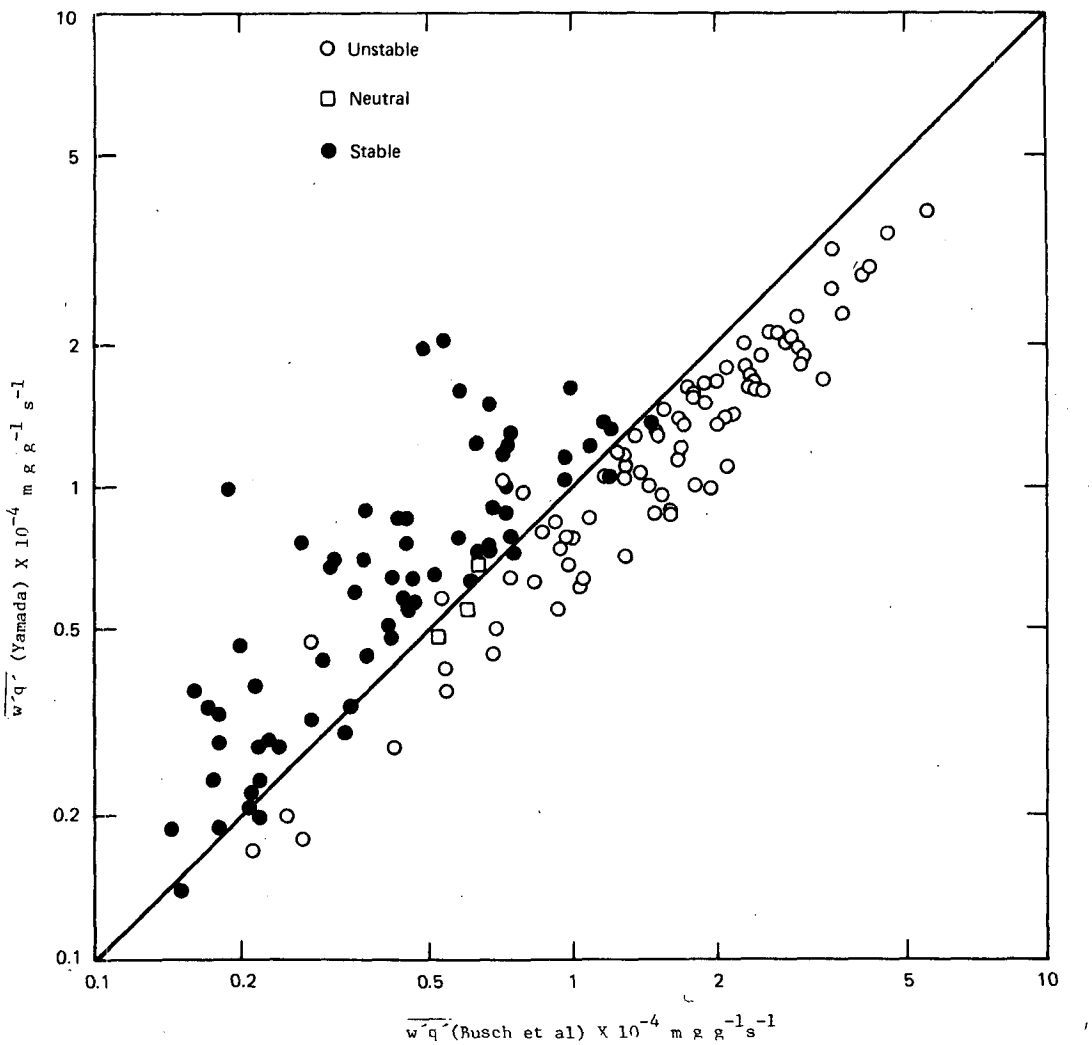

FIG. 4. As in Fig. 1 except for surface vapor flux (g g^{-1} m s^{-1}).

weak vortex, which is in gradient balance, with maximum tangential velocity of 17 m s^{-1}, embedded in a tropical atmosphere (Jordon, 1958). The lateral boundary conditions are Dirichlet for the thermodynamic variables and zero vorticity for the momentum.

For comparison purposes models were integrated using constant drag coefficients with $C_D = 0.0015$, $C_H = C_D = 0.003$ (model D1), and with $C_D = C_H = C_E = 0.003$ (model D2). A nine-layer tropical cyclone model (model M), identical to that of Anthes and Chang (1978) except for the 30 km horizontal resolution, is also integrated. The PBL parameterization in model M is that of Busch *et al.* (1976).

b. Development into tropical cyclones

The development from the initial vortex into a tropical cyclone is depicted by the maximum surface wind (Fig. 5) and minimum pressure (Fig. 6). After the initial dissipation due to friction, model S rapidly develops into an intense cyclone and reaches a quasi-steady state at ~40 h. The maximum surface wind is ~57 m s^{-1} and the minimum surface pressure is ~958 mb.

Models D1 and D2 also intensify after the initial dissipation stage. These two models deviate considerably from each other and from model S after 20 h. Model D1 reaches a final intensity of 35 m s^{-1} and 986 mb, whereas model D2 reaches a final intensity of 43 m s^{-1} and 980 mb. Model M behaves in a very similar fashion as model S, exemplified by the continuing intensification between 20 and 40 h and the final intensity of 52 m s^{-1} wind and 956 mb pressure.

c. Cyclone structure at quasi-steady state

The tangential velocity field at 48 h for Model S shows a strong and concentrated cyclonic circulation near the center (Fig. 7). The maximum velocity is at $r = 30$ km in the lowest level and the 40 m s^{-1} con-

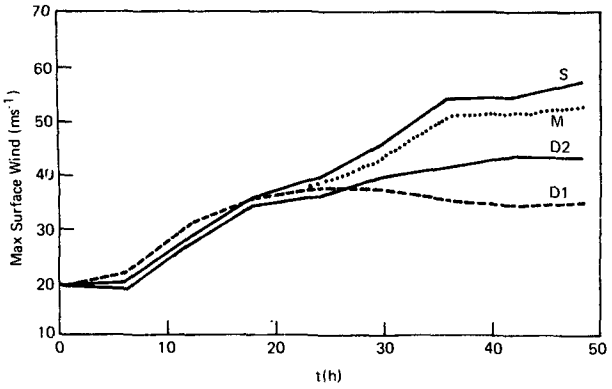

FIG. 5. Time series of the maximum winds for models S, D1, D2 and M.

tour extends upward to $\sigma = 0.6$. The tangential circulation diminishes upward due to the baroclinic effect of the warm core and anticyclonic circulation occurs at the $\sigma = 0.2$ level outside of 300 km. The inflow is confined to the PBL with maximum radial velocity of 35 m s^{-1} just outside the region of the maximum tangential velocity (Fig. 8). Strong outflow with velocity more than 20 m s^{-1} occurs at the $\sigma = 0.2$ level. Except for the shallow inflow and outflow layers, the radial velocity is small in mid-troposphere.

Fig. 9 shows the relative humidity (RH) at 48 h of model S. The RH field features (1) very moist PBL and outflow canopy, (2) relative moist convective eyewall region, (3) a dry-eye region due to the strong sinking motion, and (4) a dry mid-troposphere outside the eyewall due to the general subsidence.

The temperature field of the quasi-steady tropical cyclone shows a warm core with an anomaly exceeding +12°C (Fig. 10). The +8°C anomaly extends to $r = 300$ km in the outflow layer. The +2°C anomaly contour between $\sigma = 0.06$ and $\sigma = 0.9$ outlines the subsidence. The cooler PBL near the center is due to the adiabatic expansion (and therefore cooling) in the inflow.

d. Air-sea energy transfer

We will use budget calculations of kinetic energy, moisture and heat to compare model results and reveal the importance of various physical processes. As shown in Anthes and Chang (1978), the budgets of kinetic energy (K), moisture (Q) and enthalpy (H) for a tropical cyclone model can be expressed schematically by

$$\frac{\partial K}{\partial t} \approx K_b + C + D_v + D_L + D_H,$$

$$\frac{\partial Q}{\partial t} \approx Q_b + E + P + Q_H,$$

$$\frac{\partial H}{\partial t} \approx H_b + A + Q_p + H_s + H_H,$$

where the terms with subscript b's denote the lateral boundary fluxes, and terms with subscript H's denote the effects due to horizontal diffusion. In addition, D_V and D_C represent the rates of kinetic energy dissipation due to surface friction and cumulus friction respectively; E and P denote evaporation and precipitation rates respectively; Q_P represents latent heat release and H_s the surface sensible heat transfer; A denotes the adiabatic heating rate due to vertical motion; and C denotes the kinetic energy conversion rate due to cross-isobaric flow.

Within the model domain of $\sigma = 0$ to 1 and $r = 0$ to 300 km, the most direct contribution of the PBL processes are the air-sea sensible and latent heat exchanges. Figs. 11 and 12 show the time series of H_s and E. During the early stages, the sensible and latent heat transfers of D1 are equal or greater than

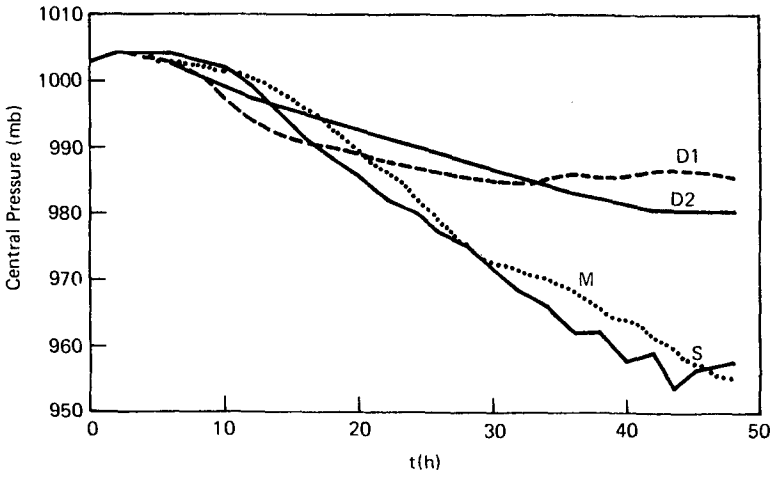

FIG. 6. Time series of the minimum surface pressures for models S, D1, D2 and M.

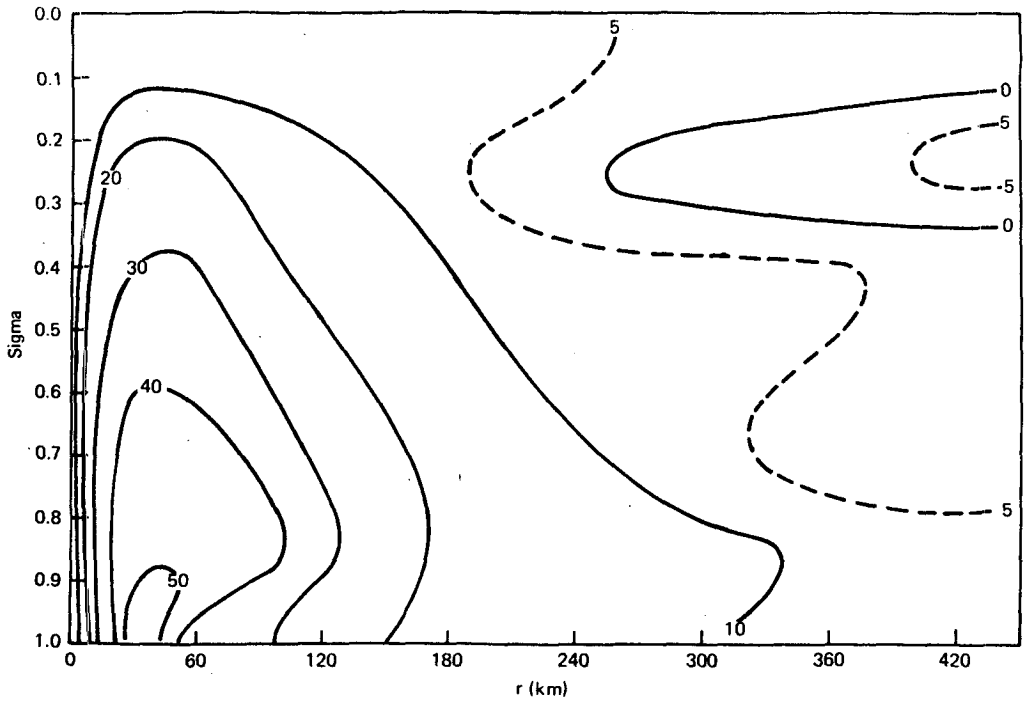

FIG. 7. The quasi-steady tangential velocity (m s^{-1}) of model S at 48 h. Positive values denote cyclonic circulation, negative values denote anticyclonic circulation.

those of S. The sensible and latent heat exchanges in S, however, grow steadily after 10 h and finally reach 15×10^{12} W and 3 cm day^{-1}, respectively, whereas in D1, the sensible and latent heat exchanges only grow to maxima of 7.5×10^{12} W and 1.8 cm day^{-1} after 30 h. After the maxima are reached, they

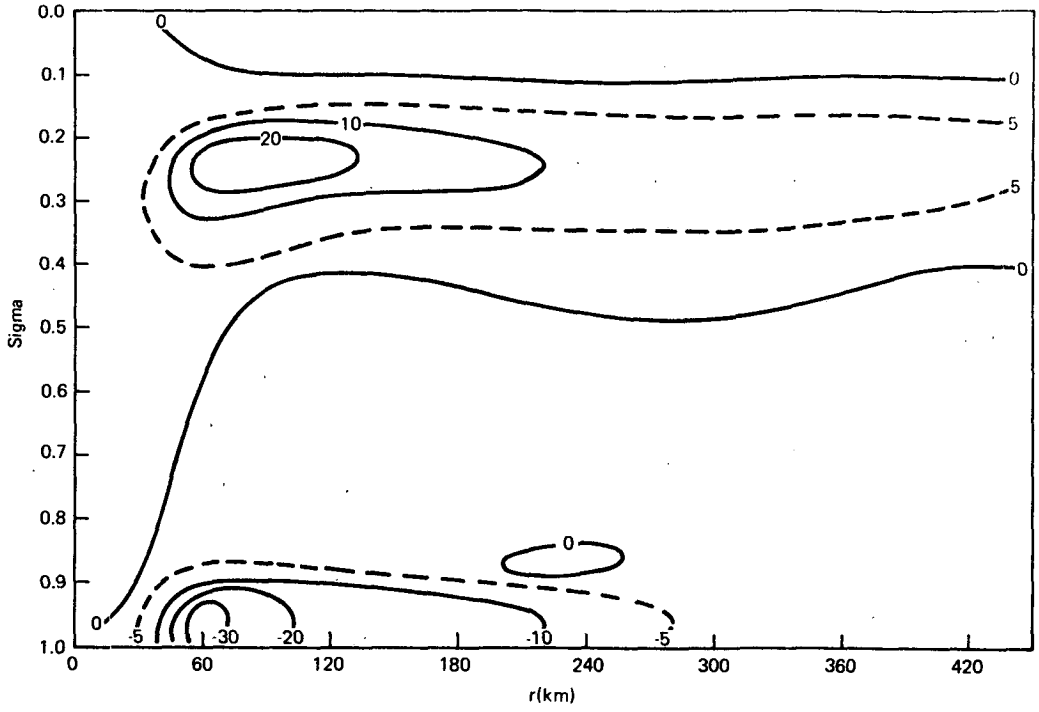

FIG. 8. The quasi-steady radial velocity (m s^{-1}) of model S at 48 h. Positive values denote outflow, negative values denote inflow.

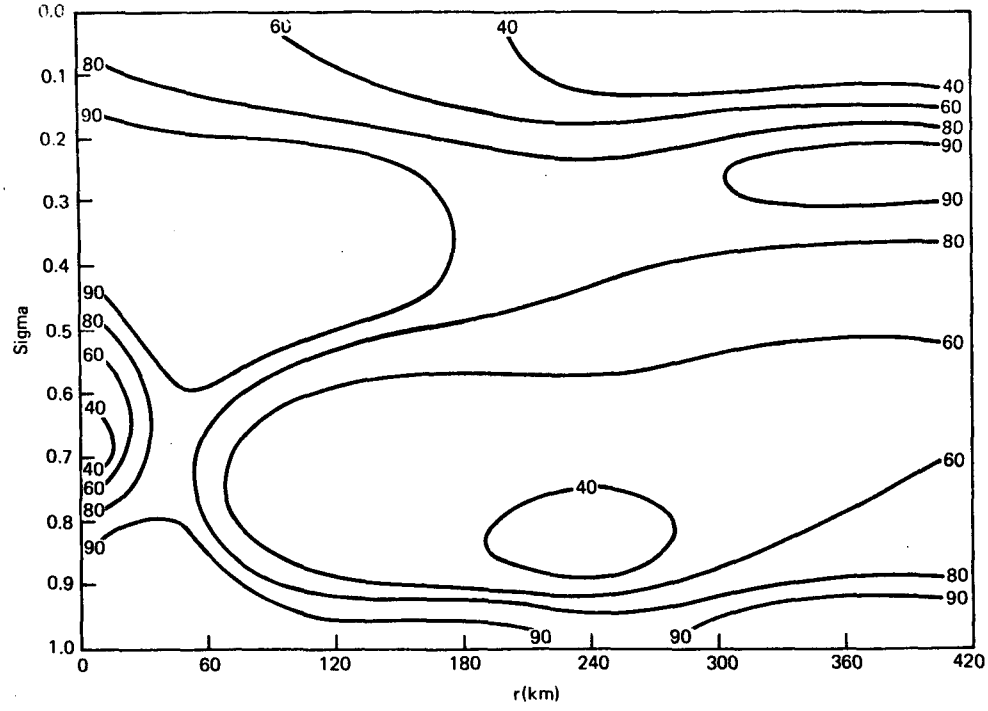

FIG. 9. The quasi-steady relative humidity (%) of model S at 48 h.

decrease with time because of stabilization and saturation of the PBL.

Apparently, the sensible and latent heat exchanges in S are maintained at high levels primarily due to their nonlinear dependence on wind speed and stability. As wind speed in S approaches its maximum

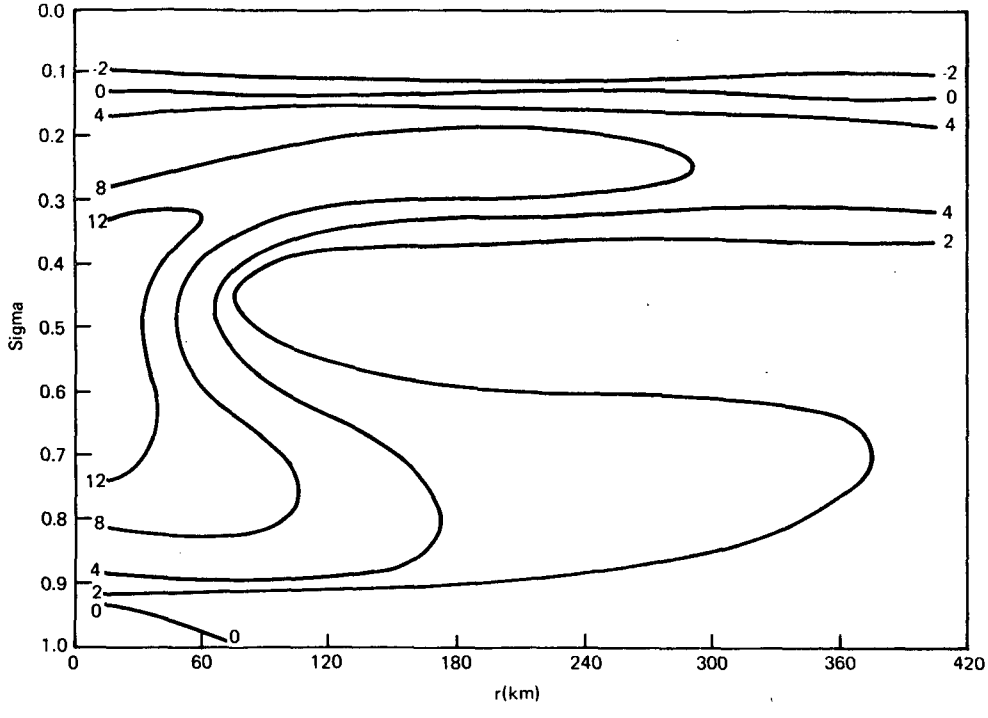

FIG. 10. The quasi-steady temperature anomalies (C) of model S at 48 h. The anomalies are defined as temperature departures from the initial state.

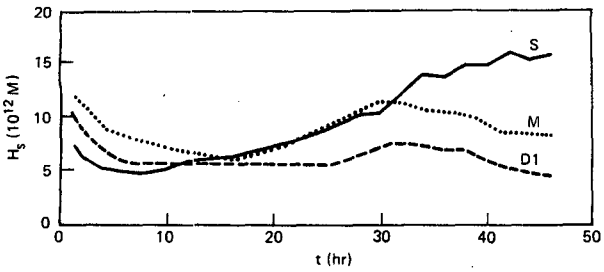

FIG. 11. Time series of surface heat flux from r = 0 to 300 km of models S, D1 and M.

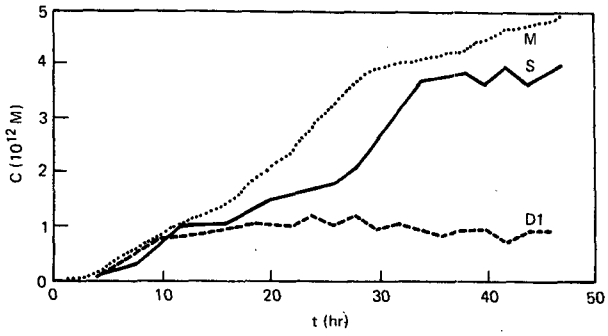

FIG. 13. As in Fig. 11 except for kinetic energy conversion rate.

after 30 h, both H_s and E are enhanced to a greater extent than in D1. In addition, the radial circulation in S also is increased so that a slightly unstable and dry PBL is maintained by the strong inflow.

The time variation of E for model M is very close to model S. The sensible heating rate H_s, however, are very different. This is because in model M a downward heat flux across the PBL top is allowed. Anthes and Chang (1978) argued this as an alternative heat source for maintaining the quasi-isothermal hurricane PBL. The GSA does not consider the across inversion mising, therefore Model S depends on extracting sensible heat from the ocean to maintain its quasi-isothermal inflow layer.

The increased radial circulation is illustrated by the conversion rate C from the available potential energy to kinetic energy shown in Fig. 13. The conversion rate is approximately proportional to the combined strength of the radial circulation and the warm core. It is apparent that the conversion rates in model S and M grow rapidly between 10 to 20 h, which coincides with the increased evaporation. The proportionally faster increase of C than H_s and E in model S shows that the increased heat transfer creates a stronger inflow, which, in turn, maintains a stronger heat transfer and a stronger inward transport of the dry, cooler ambient air.

The two different PBL parameterizations also gives different dissipation rates (Fig. 14). Note that D_V in S is smaller before 15 h than in D1, and it eventually asymptotes to three times stronger. Again, this is due to the nonlinear dependence of the surface stress on wind speed.

One can argue that the nonlinear dependence of the air-sea energy exchange could be achieved by employing wind-speed-dependent drag coefficients. However, the parameterization based on similarity theory has greater merit. The heat and momentum transfers depend not only on wind speed but also on PBL stability, and it is through PBL stability that various fluxes are correlated. The surface roughness appears in the formulation as a length scale and thus the parameterization captures an important feedback from the sea state. The turning of wind in low levels, neglected in the parameterization with drag coefficient, it also included implicitly. Therefore, the surface stress backs from the direction of the PBL mean wind, as expected.

Overall, the generalized similarity theory is quite similar in estimating surface fluxes to the more sophisticated Busch *et al.* model and appears to be applicable in parameterization of the PBL in the tropical cyclone models. Such parameterization contains several realistic PBL characteristics such as the mutual dependence of various fluxes and the backing of the low-level wind. Although it cannot resolve the strong gradient in a stable PBL nor the across-inversion mixing in some single-layer parameterizations, it is still superior than the parameterization using stability independent drag coefficient. In cases that a multilayer parameterization is economically infeasible, the parameterization outlined by (3) is a good alternative.

5. Summary

A PBL parameterization based on the generalized similarity theory has been tested for tropical cy-

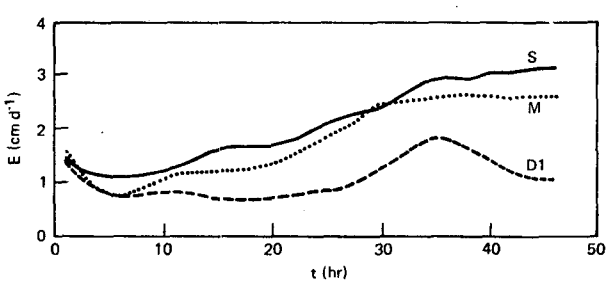

FIG. 12. As in Fig. 11 except for averaged evaporation rate.

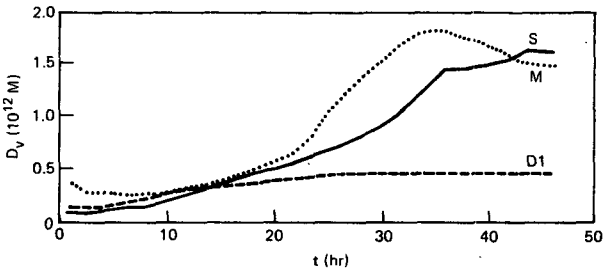

FIG. 14. As in Fig. 11 except for kinetic energy dissipation rate due to surface friction.

clone models. We conclude that a single-layer approach in parameterizing the PBL is viable although it cannot resolve the detailed structure of the PBL.

This parameterization was compared with the one-dimensional multilevel PBL model of Busch *et al.* (1976) under various stabilities and highly nonstationary conditions. For stationary conditions, the computed water vapor flux, agrees well with the Busch model. The momentum flux is overestimated and the sensible heat flux is underestimated especially when there is a low-level inversion.

An axisymmetric tropical cyclone model which incorporated this single-layer parameterization produced very realistic dynamic and thermodynamic structures. In comparison with otherwise identical tropical cyclone models that employ constant drag coefficients, the superiority of stress-dependent drag coefficients in the development of tropical cyclones was demonstrated.

Acknowledgments. The author thanks Dr. R. V. Madala for his support, and Drs. M. R. Schoeberl, D. F. Strobel and R. T. Williams for comment on the manuscript. Sharon Richardson and Jane Polson diligently typed the manuscript. The research is supported by the Naval Research Laboratory through Grant N00173-78-C-0421.

REFERENCES

Anthes, R. A., and S. W. Chang, 1978: Response of the hurricane boundary layer to changes of sea surface temperature in a numerical model. *J. Atmos. Sci.*, **35**, 1240–1255.

——, and T. T. Warner, 1978: Development of hydrodynamic models for air pollution and other mesometeorological studies. *Mon. Wea. Rev.*, **106**, 1045–1078.

Arya, S. P. S., 1978: Comparative effects of stability, baroclinicity and the scale-height ratio on drag laws for the atmospheric boundary layer. *J. Atmos. Sci.*, **35**, 40–46.

——, 1977: Suggested revisions to certain boundary layer parameterization schemes used in atmospheric circulation models. *Mon. Wea. Rev.*, **105**, 215–227.

Busch, N. E., S. W. Chang and R. A. Anthes, 1976: A multi-level model of the planetary boundary layer suitable for use with mesoscale dynamic models. *J. Appl. Meteor.*, **15**, 909–919.

Businger, J. A., J. C. Wyngaard, Y. Izumi and E. F. Bradley, 1971: Flux profile relationships in the atmospheric surface layer. *J. Atmos. Sci.*, **28**, 181–189.

Deardorff, J. W., 1972: Parameterization of the planetary boundary layer for use in general circulation models. *Mon. Wea. Rev.*, **100**, 93–106.

Delsol, F., K. Miyakoda and R. H. Clarke, 1970: Parameterized processes in the surface boundary layer of an atmospheric circulation model. *Quart. J. Roy. Meteor. Soc.*, **97**, 181–208.

Jordan, C. L., 1958: The thermal structure of the core of tropical cyclones. *Geophysics*, **6**, 218–297.

Kurihara, Y., and R. E. Tuleya, 1974: Structure of a tropical cyclone developed in a three-dimensional numerical simulation model. *J. Atmos. Sci.*, **31**, 893–919.

Moss, M. S., and F. J. Merceret, 1976: A note on several low-layer features of Hurricane Eloise (1975). *Mon. Wea. Rev.*, **104**, 967–971.

Pielke, R. A., 1974: A comparison of three-dimensional and two-dimensional numerical predictions of sea breezes. *J. Atmos. Sci.*, **31**, 1577–1585.

Rosenthal, S. L., 1971: The response of a tropical cyclone model to variations in boundary layer parameters, initial conditions, lateral boundary conditions, and domain size. *Mon. Wea. Rev.*, **99**, 767–777.

Yamada, T., 1976: On the similarity functions *A*, *B* and *C* of the planetary boundary layer. *J. Atmos. Sci.*, **33**, 781–793.